PHOTOMETRY OF LATE TYPE STARS

Lowell R. Doherty
University of Wisconsin
Madison, Wisconsin

I. INTRODUCTION

OAO-2 was launched December 7, 1968 carrying optical ultraviolet instrumentation of SAO and the University of Wisconsin. A description of the Wisconsin Experiment Package has been published elsewhere (Code et al. 1970). Here we present broad-band filter photometry for 57 bright stars of spectral type A2 and later observed between February 1969 and October 1970. Four filter bands are discussed with peak instrument response at 3320, 2980, 2460 and 1910 Å. The data include nearly all usable filter observations of G, K and M types. Sampling is nearly complete for A and F giants and supergiants, with the exception of Cepheid variables, which are not included here. Only a few representatives of the A and F main sequence were selected.

The basic results presented here are relative digital counting rates obtained with a field-stop aperture of 10 minutes of arc. Characteristics of the four filter-photometer combinations and errors are discussed in § II. Because the aperture is large, and the contrast between stars of different spectral type is dramatically increased in the ultraviolet, some observations require substantial correction if they are to represent the visually brightest star in the field. Possible corrections of $0^{m}.01$ or more due to identified secondary stars must be considered for one-third of the pointings. These corrections and the effects of interstellar reddening are discussed in § III. The adjusted counts are then used (§ IV) to construct color-color diagrams and are compared to the recent SAO grid of model atmospheres.

II. PHOTOMETRY

Each of the four 8-inch stellar telescopes aboard OAO-2 has a filter wheel with three interference filters, a Sr^{90} calibration source and a dark position. Thus there are 12 filter-photometer combinations labelled, e.g. S1F1 (Stellar 1, Filter

1). All filters are used in the first order. In his study of planetary albedoes derived from OAO data, Caldwell (1970) found systematic differences between filters which he attributed to pin hole defects in S2F1 (2030 Å) and S2F5 (2390 Å). Proximity to the calibration source appears to affect S3F5 (1680 Å). S2F2 (2940 Å) is erratic for as yet unknown reasons. We have chosen not to include data from these filters here. Of the remaining ultraviolet bands, Stellar 4 (1200-1700 Å) provides very little data for this spectral range and will not be included. The four bands used here are S1F1 (3320 Å), S1F4 (2980 Å), S3F1 (1910 Å) and S3F2 (2460 Å). They appear to be quite stable. Stellar 3 is particularly well suited to photometry of late type stars because its Ascop 541F photomultiplier is insensitive longward of 3500 Å. Stellar 1 employs an EMI 6256, whose response extends well into the red. S1F1 includes a UG11 filter to reduce this response, while S1F4 does not.

One "observation" typically consists of a sequence of measurements with all filters and various integration times. The minimum set of data or data output frame provides 24 individual measurements. These consist of, for each photometer, 6 successive integrations over the same time interval at one filter wheel position. These times need not be and usually were not the same for all photometers. Integration times used were 1/8, 1, 8 and 64 seconds. A spacecraft counter truncates the data before storage and eventual transmission to the ground. One count in the output equals 64 photomultiplier events. Hereafter, any reference to a specific number of counts means OAO (reduced) counts.

Errors in the photometry arise principally in variations in instrument sensitivity and dark noise. CAL (radioactive source) readings show variations in sensitivity of one or two percent over several orbits and larger variations up to about ten percent over months of operation. Long-term changes presumably depend on the spacecraft environment. To account for such changes the data are reduced according to the scheme:

$$R = \left(\frac{\text{STAR-DARK}}{\text{CAL-DARK}}\right)_i T_i - \left(\frac{\text{SKY-DARK}}{\text{CAL-DARK}}\right)_k T_k \ . \qquad (1)$$

$T = T(t)$ corrects for the decay of the source. Small CAL-DARK differences from one orbit to the next may also be environmental or may simply reflect differences in positions of the filter wheels. It was discovered early in OAO operation that rapid, extreme changes in DARK occur near the South Atlantic Anomaly in the earth's radiation belts. We now know that no part of the orbit is free of contamination. Later observations have avoided the region of the Anomaly entirely and include more DARK readings. Nevertheless, our information about how DARK

varies with time is poor. The spacecraft typically moves through a quarter of the earth's circumference during an observational sequence that may include DARK at only one or two positions. Variations in STAR within one frame and between frames serve as a guide, but both changes in DARK and sensitivity may be involved.

At present it does not appear feasible to program the full data reduction. Here each frame has been treated individually and suspicious data discarded according to our judgment. In any sequence with low, reproducible DARK Stellar 1 counts are repeatable to the photon noise limit of one percent or better. Different orbits reproduce less well. For three observations of η Cas (3.4 G0 V) made over some ten orbits, the spread in the data is less than one percent. However, the spread is two percent for three observations of η Dra (2.7 G8 III) made over ten orbits, and this increases to four percent if we include a fourth observation of η Dra made several hundred orbits earlier. Good Stellar 3 frames have the same high internal consistency as Stellar 1 for all but the faintest ultraviolet objects. For later spectral types with low counting rates, the ambiguity due to integer counts can be important. Data has also been extracted from some sequences with variable DARK or minimal information. This is possible where information from neighboring orbits helps to estimate the degree of contamination. Often a SKY sequence identical to the stellar observation follows in the next orbit and a constant DARK difference can be applied to all frames.

The first term in equation (1) is probably determined to ±2 percent for all Stellar 1 observations, for A, F and G stars at 2460 Å, and for A and F stars at 1910 Å. Exceptions to this general rule will be mentioned later. Net SKY counts at galactic mid-latitudes mimic a 10th magnitude F star. Thus the second term in equation (1) becomes important for the fainter G stars and for all K and M stars. Again with exceptions, the error in R for K and M stars at 2460 Å is probably within ±10 percent.

Table 1 contains the basic data. Where possible, UBV are taken from Iriarte *et al.* (1965). Other principal sources are Cousins and Stoy (1963) and the Naval Observatory catalog (Blanco *et al.* 1968). C_λ has the same value for all entries in a single column. Its purpose is to make equal entries correspond approximately to equal flux per unit wavelength at the nominal wavelengths. This correspondence is approximate for two reasons. First, the calibration is based on model atmospheres of early type stars rather than laboratory sources. Conventional laboratory sources are subject to large systematic errors in the ultraviolet. Using synchrotron radiation from a storage ring, as described elsewhere in this volume by Bless and Fairchild, should eventually provide much more accurate calibration of the OAO photometry. Until this is possible, however, it has proved useful at SAL to adopt an absolute cali-

Table 1. Observations

HD	Name	Spectral Type	V	U-V	B-V	2.5 Log $R_\lambda + C_\lambda$ 3320	2980	2460	1910	Remarks
1522	ι Cet	K2 III	3.55	2.39	1.22	-0.10	-1.13	-3.61		
1581	ζ Tuc	G2 V	4.22	0.59	0.58	1.34	0.87	-0.46	-1.84	
2151	β Hyi	G1 IV	2.79	0.72	0.62			0.56	-1.08	
3712	α Cas	K0 II-III	2.22	2.30	1.17	1.35	0.35	-2.20		S
4614	η Cas	G0 V	3.43	0.62	0.58	2.12	1.63			
6178	σ Scl	A2 V	5.50	0.21	0.08	0.44	0.37	0.29	0.71	S
6860	β And	M0 III	2.04	3.53	1.57	0.14	-0.83	-3.59		S
8538	δ Cas	A5 V	2.69	0.28	0.13	3.03	2.96	2.78	3.17	
9053	γ Phe	K5 II	3.40	3.40	1.56	-1.10	-1.91	-3.27	-4.14	S
11443	α Tri	F6 IV	3.44	0.57	0.49	2.16	1.81	0.69	-0.77	
11937	χ Eri	Gv IV	3.70	1.31	0.85	0.96	0.28	-1.75	>-4.29	
12929	α Ari	K2 III	2.00	2.27	1.15	1.60	0.57	-2.44	-4.13	
13161	β Tri	A5 III	3.00	0.30	0.16	2.74	2.70	2.07	2.32	
13174	14 Ari	F2 III	4.99	0.34	0.34	0.62	0.32	-0.46	-0.69	S
29129	α Tau	K5 III	0.86	3.50	1.55	1.26	0.18	-2.77	-4.41	S
31964	ε Aur	F0 Ia	3.00	0.86	0.54	1.64	1.09	-0.38	-0.96	S,0.20
36079	β Lep	G5 III	2.81	1.31	0.82	1.93	1.27	-0.72	-2.59	
38393	γ Lep	F6 V	3.60	0.44	0.48	2.14	1.76	0.65	-0.42	
39801	α Ori	M2 Ib	0.69	3.92	1.86	0.99	0.21	-1.50	<-3.33	1.64
48329	ε Gem	G8 Ib	2.98	2.87	1.40	-0.01	-0.84	-3.06		S,1.03
56986	δ Gem	F0 IV	3.52	0.40	0.34	2.14	1.93	1.12	1.20	
68457	56 Cam	A7 V	6.45	0.31	0.20	-0.76	-0.90	-1.24	-1.14	
72905	π^1 UMa	G0 V	5.63		0.61	-0.24	-0.74	-2.21	-3.55	
76644	ι UMa	A7 V	3.15	0.27	0.19	2.76	2.67	2.37	2.47	
82210	24 UMa	G4 IV	4.56	1.11	0.77	0.37	-0.27	-2.09	-3.77	
82328	θ UMa	F6 IV	3.20	0.52	0.46	2.45	2.10	1.05	0.16	
84441	ε Leo	G0 II	2.98	1.27	0.81	1.78	1.08	-0.77	-2.44	0.70

106591	δ UMa	A3	V	3.33	0.15	0.08	2.60	2.60			
108903	γ Cru	M3	II	1.66	3.37	1.61	0.77	0.95?	-0.74	-0.52	S
124897	α Boo	K2	III	-0.06	2.52	1.24	3.39	2.17	-0.76	-0.81	
128620	α Cen	G2	V	-0.01		0.68			2.89	1.03	S
128898	α Cir	F0	V	3.18	0.34	0.24	2.57	2.46	2.17	2.09	
129078	α Aps	K5	III	3.82	3.11	1.44	-1.46:		-4.78		S
139063	υ Lib	K5	III	3.58	2.97	1.38	-0.80	-1.88	-4.50		S
147675	γ Aps	K0	IV	3.88	1.53	0.91			-2.28	-3.90	
148387	η Dra	G8	III	2.74	1.61	0.91	1.66	0.87	-1.46	-3.34	S
148856	β Her	G8	III	2.77	1.63	0.94	1.63	0.90	-1.11		
150680	ζ Her	G0	IV	2.81	0.86	0.66	2.47	1.93	0.27	-1.54	
150997	η Her	G7	III-IV	3.50	1.53	0.92	1.05	0.28	-1.93	-4.16	
159181	β Dra	G2	II	2.78	1.63	1.00	1.59	0.93	-0.80	-2.32	0.85
163506	89 Her	F2	Ia	5.44	0.65	0.34	-0.59	-0.99	-2.86		S,0.25
163588	ξ Dra	K2	III	3.75	2.40	1.18	-0.33	-1.33	-4.44		
164058	γ Dra	K5	III	2.23	3.39	1.51	0.06	-1.02	-4.82		
165341	70 Oph	K0	V	4.05	1.35	0.84	0.68	-0.05	-2.49		S
170153	χ Dra	F7	V	3.57	0.44	0.48	2.16	1.84	0.60	0.10	
180711	δ Dra	G9	III	3.07	1.78	1.00	1.14	0.24	-2.33		
185395	θ Cyg	F4	V	4.49	0.34	0.37	1.33	1.04	0.22	-0.31	S
197345	α Cyg	A2	Ia	1.25	-0.15	0.09			4.03	4.38	
197989	ε Cyg	K0	III	2.46	1.91	1.03	1.56	0.82	-2.04	-3.89	
200905	ξ Cyg	K5	Ib	3.70	3.45	1.65	-1.66	-1.86	-3.85	-4.48	
202109	ζ Cyg	G8	II	3.19	1.76	1.00	1.07	0.41	-2.58		
207260	ν Cep	A2	Ia	4.29	0.64	0.51	0.86	0.48		-3.06	S,0.05
210459	π Peg	F5	II	4.27	0.66	0.48	1.00	0.62	-0.42	-1.10	0.37
210745	ζ Cep	K1	Ib	3.36	3.27	1.55	-0.88	-1.67	-4.60	-4.91	S,1.18
217906	β Peg	M2	II-III	2.42	3.62	1.67			-4.28		S
222107	λ And	G8	III-IV	3.75	1.74	1.01			-2.22		
222404	γ Cep	K1	IV	3.21	1.98	1.03	0.73	-0.26	-2.92	-5.64	

bration for preliminary interpretation of the data. A. D. Code (private communication) derived values of C_λ by comparing filter observations of unreddened early B stars with models by D. C. Morton. These values are listed in Table 2 and have been incorporated in the SAL data reduction program, DROOP. The second reason that entries in Table 1 do not represent the actual flux at the nominal filter wavelengths is that no correction for changes in effective wavelength with different spectral type have been included.

Table 2. Absolute Calibration Constants

λ	1910	2460	2980	3320	U	V
C_λ	4.11	2.04	0.31	0.00	-6.09	-6.14

Remarks are of two kinds: the letter S means that secondary field stars may be important, and the named star is therefore also listed in Table 3. A number in the remark column is the intrinsic B-V value (Johnson 1966) for the spectral type of the named star. Intrinsic colors are included only for stars with excesses greater than about $0^m.1$.

III. CORRECTIONS FOR FIELD STARS AND REDDENING

The photometers are equipped with both 2 and 10 minute of arc stops, but the smaller aperture has been used sparingly. This policy is aimed to minimize the chance that a malfunction would leave the smaller stop permanently in position. Even slightly poorer pointing stabilization would make that photometer useless. All of the observations reported here used the 10 minute stop. Uncertainties in spacecraft pointing, alignment of the optical axes of the stellar telescopes, and image size make it impossible to identify all secondary stars exactly. Moreover, spectral type and reddening for the fainter secondary stars are not accurately known. Secondary stars listed in Table 3 are those ADS and DM stars which may contribute one percent or more of the total flux. To select these stars we have supposed that the center of the field aperture may be displaced up to 2 minutes. Thus stars within a radius of 7 minutes were examined, but not all of these can necessarily be seen at the same time. For most faint stars, visual magnitudes and spectral types taken from the SAO Catalog (1966) were used to compute fluxes without correction for reddening. As will be shown in § IV, ultraviolet fluxes correlate well with B-V. Tabulated spectral types were converted to colors according to Johnson

(1966). Where no spectral type is available, we have used the earliest type consistent with available visual and ultraviolet data. We assume, however, that types earlier than A are unnecessary because they are strongly reddened in this visual magnitude range.

Table 3 lists the corrections, in magnitudes, to be applied to the corresponding fluxes in Table 1. In some cases the corrections are quite large. We have included these because very little data would otherwise be available for the latest spectral types. Some stars in Table 3 require individual comment:

γ Phe: the computed secondary flux at 1910 Å is approximately that observed.

ε Gem: correction assumes only one 7 minute star in the field with 1910 Å flux equal to the detection limit (approximately type A).

γ Cru: Cousins and Stoy (1963) give B-V = 0.16 for the secondary, which seems red for A2. Fluxes were computed for an unreddened star of this color and a reddened star with B-V = 0.08. The resulting 2460 Å primary fluxes differ by a factor of two. The tabulated correction refers to the mean. For 1910 Å the correction based on an unreddened secondary is tabulated. This gives an approximate upper limit to the γ Cru flux since the reddened secondary leaves no net flux.

α Cen: α^2 photometry from Gliese (1969).

α Aps: the 6 minute secondary is probably not in the field; if the 5 minute secondary is F, it can account for the total observed flux at 2460 Å.

Interstellar extinction in the ultraviolet is complex. Bless and Savage (1972) have discussed the OAO reddening data in detail. Here we will use a mean reddening curve. For the color ratios $E(\lambda-V)/E(B-V)$, we adopt the values 1.8 (3320 Å), 2.15 (2980 Å), 3.0 (2460 Å) and 5.0 (1910 Å).

IV. DISCUSSION

The narrow band photometry of Mitchell and Johnson (1969) includes a band labelled "33" whose peak response, at 3370 Å, nearly coincides with S1F1. We will define "3320" as an arbitrary magnitude whose value is the negative of the entry in Table 1. Figure 1 plots 3320-33 against B-V. Vertical bars show the uncertainty due to secondary stars near the edge of the field. The very discrepant point at B-V = 1.65 is ξ Cyg. Although the original data look perfectly good, Figure 1 and subsequent comparisons suggest that 3320 for this star is wrong. The scatter in Figure 1 does not depend strongly on color. However, the points fill a band about $0^m.2$ wide, which is greater than internal errors lead us to expect (§ II). We will see below (Figures 2 and 3) that $\pm 0^m.02$ is a realistic estimate of 3320 error for all but a few stars. Thus most of the scatter

Table 3. Corrections for Secondary Stars

Pri	Sec	Separation (arc min)	m_v	Spectral Type	Δm 3320	2980	2460	1910	Remarks
α Cas	+55 138	1	8.8	K0	.01	.01	:02		
σ Scl	-32 406	5	8.8	F8	.045	.03	.01		max
β And	+34 199	6	8.6	F5	.08	.145	.91		max
γ Phe	-43 451	1	8.5	F0	.295	.555	1.33		1910≃obs
14 Ari	+25 354	2	8.6	F2	.05	.05	.05	.03	
α Tau	+16 628	7	9.3	?	.01	.03	.30		1910≃obs
	+16 630	2	9.5	?					
ε Aur	+43 1168	3	9.0	K?	.025	.05	.12	.81	max
	+43 1170	6	8.6	A0					
γ Lep	BS 1982	2	6.4	G5	.06	.045	.03	.02	min
	-22 1217	6	8.0	A0	.08	.08	.11	.46	max
ε Gem	+25 1407	2	9.0	K2	.015	.015	.01		min
	+25 1400	7	9.5	?	.055	.085	.32		max
	+25 1403	7	9.5	?					
	+25 1404	7	9.4	?					
γ Cru	BS 4764	2	6.41	A2	.365	.275	2.35	1.85	1910=obs?
α^1 Cen	α^2 Cen	9"	1.33	K0			.07	.06	B-V = 0.88
α Aps	-78 890	6	9.0	A?					2460>>obs
	-78 891	5	9.4pg	?	.25				2460 ≅ obs
υ Lib	-27 10459	7	9.9	?	.05	.12	.31		max
	-27 10468	7	9.8	?					
η Dra	ADS	5"	8	K1	.01	.01			
89 Her	+26 3118	5	9.2	F2	.09	.10	.26		max
70 Oph	ADS	4"	6.0	K5	.065	.05	.02		
θ Cyg	BS 7465	5	6.5	G9 III	.055	.065	.04	.08	max
	R Cyg	4	6.5	S4					
	+49 3065	4	9.0	A5					
ν Cep	+60 2290	5	8.4	G0	.035	.03		.06	max
ζ Cep	+57 2472	6	9.3	B(11.4pg)					assume negl.
β Peg	ADS	4	9.4	?			.96		max

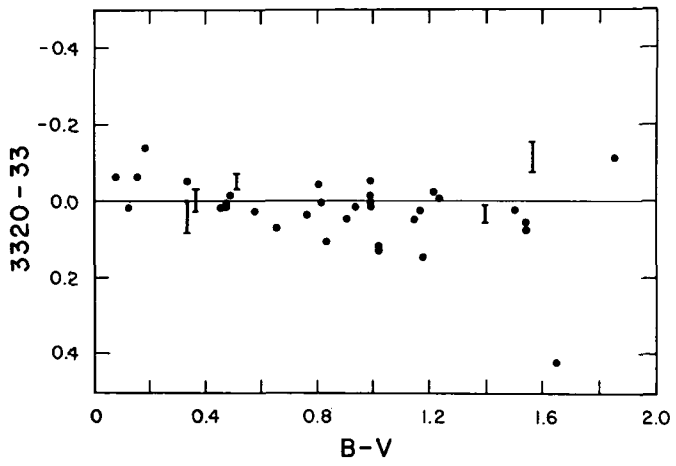

Figure 1.—OAO 3320 filter magnitudes minus Mitchell and Johnson 33 band. Zero point arbitrary.

in Figure 1 must be attributed to the ground-based photometry.

In the several color-color diagrams below, five luminosity classes are distinguished by different graph symbols. Secondary corrections have been applied according to Table 3. Stars with intrinsic B-V given under Remarks in Table 1 have been adjusted according to the mean reddening ratios of § III and are plotted at their unreddened positions. All colors except B-V have been plotted on an absolute scale. For colors that involve V or U, this required zero-point shifts C_V and C_U in addition to the C_λ already described. C_V is defined by the equation

$$\delta m = 3320\text{-}V\text{-}C_V \quad ,$$

where δm gives the ratio of the flux per unit wavelength at 3320 Å to the flux at 5500 Å. C_V and C_U, which is similarly defined, are given in Table 2. Figure 2 plots 3320-U against B-V. Main sequence and subgiant stars between θ UMa (F6 IV, B-V = 0.46) and γ Cep (K1 IV, B-V = 1.03) show a remarkably tight color correlation. If we allow errors up to $0^m.02$ in both colors all of these points can be placed on the curve shown, which for discussion purposes we have extrapolated to M0. Yellow and red giants together define a roughly parallel sequence. The four stars well below this sequence are probably misplaced. The giant is α Aps, for which 3320 is uncertain due to the radiation belt. ξ Cyg is discrepant in the same sense as in Figure 1, and by about the same amount. The remaining supergiants are γ Phe and γ Cru, both very red, deep southern objects whose V magnitudes may be systematically different from the bulk

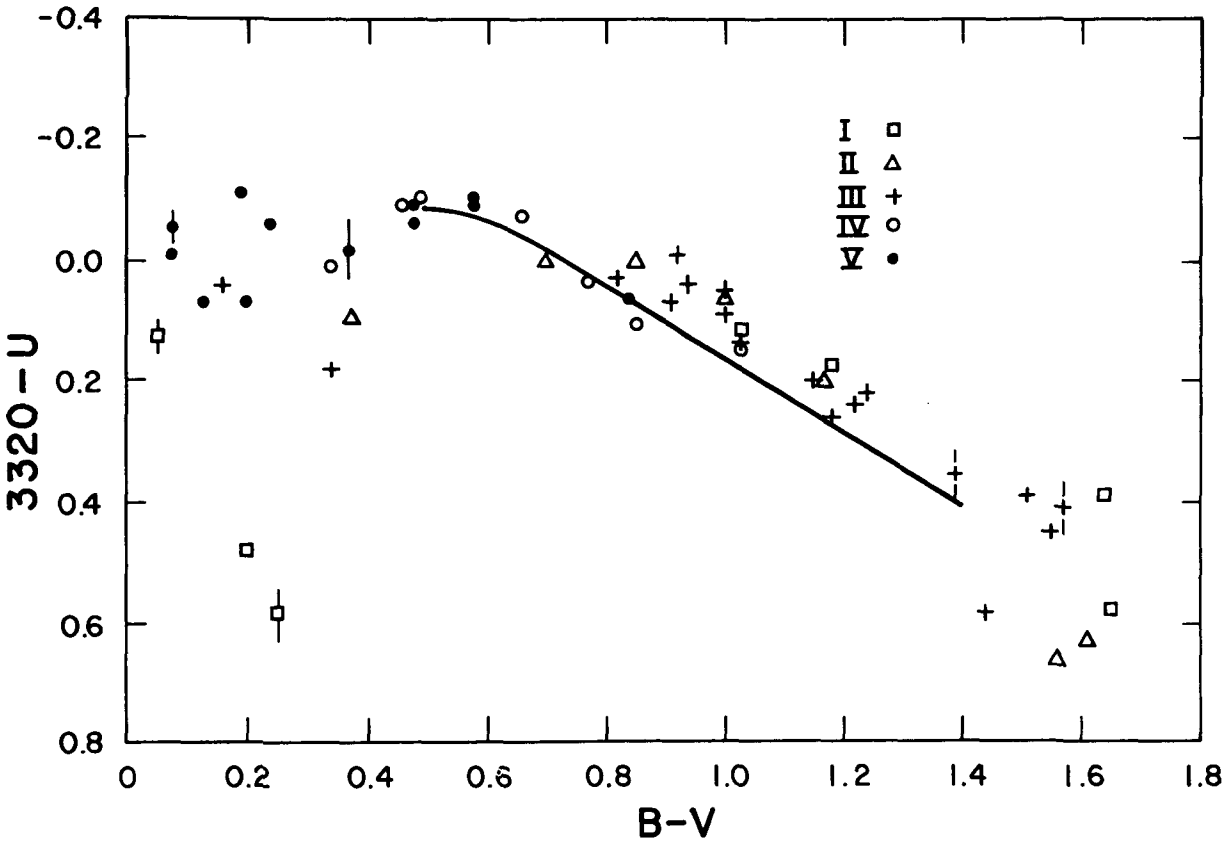

Figure 2.—3320-U vs. B-V with colors corrected for secondary stars and reddening. Ordinate zero point corresponding to equal flux per unit wavelength. The line shows extrapolated dwarf sequence.

of stars here.

Figure 3 makes use of two OAO magnitudes, 2980 and 3320. Their differences should be independent of all but very rapid changes in photometer characteristics (except filter deterioration). Again, class IV and V stars show excellent correlation with B-V. This is not surprising for the earlier spectral types, where the relation involves essentially the slopes of the Balmer and Paschen continua, i.e. the relation is not a strong function of temperature and gravity. It is worth mention for the cooler stars in which the source function is more sensitive to temperature and in which line opacity plays a greater part. Notice the clear separation of a class I sequence but almost no discrimination between II and III. According to Figure 1, ξ Cyg should be lowered about $0^{m}.4$ from its position in the upper right corner of Figure 3. Stars with

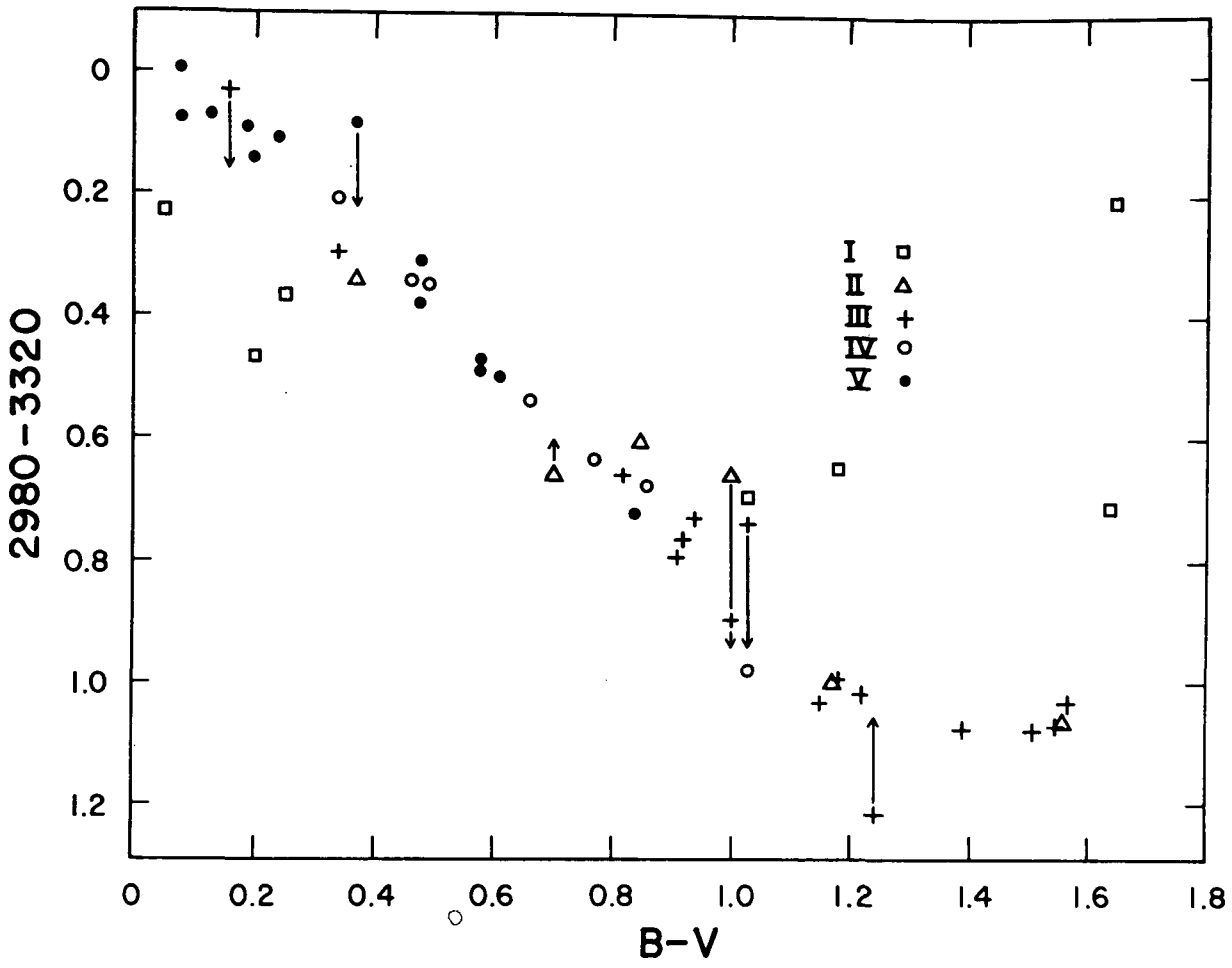

Figure 3.—2980-3320 vs. B-V with corrected colors and ordinate zero shift as in Figure 2. Arrows indicate possible corrections due to photometric errors, as discussed in text.

arrows probably have ξ Cyg type errors. Ignore the arrows for the moment.

Two features of Figure 3 persist over the broader color base 2460-V, which is plotted in Figure 4. The main sequence is well defined, especially at F and G. The class I separation is present but not as clear cut. Reddening errors could obscure a smoother relation among these supergiants if one exists, since ε Aur, ε Gem and ζ Cep have apparent excesses greater than $0^m.3$ in B-V and 1^m in 2460-V. The lower part of Figure 4 resembles a fan with its apex an F star. At least some of this spreading is luminosity-dependent. Identify the position of a point in the fan by the slope of the line joining the point to the apex.

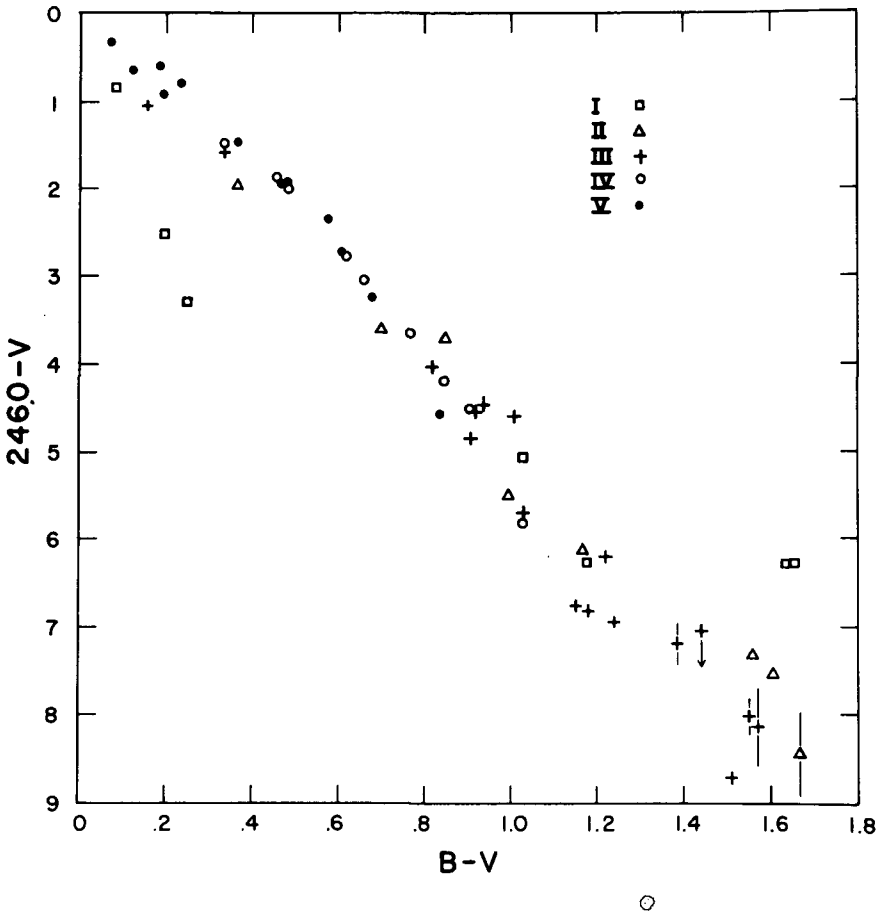

Figure 4.—2460-V vs. B-V with corrected colors and ordinate zero shift as in Figure 2.

Take the position of the apex arbitrarily as 2460-V = 2.1 and B-V = 0.54. Figure 5 compares this slope with M_V determined from the width of the Ca II K emission (Wilson and Bappu 1957). Only stars with B-V > 0.8 are included. One-third of these do not have K-line luminosities. Class I stars are plotted according to their observed colors. Depending on the exact slope of the reddening line, these stars can go up or down. Note that M_V = -5.7 for β Dra, +1.2 for ζ Cyg and -1.2 for ι Cet, in disagreement with their spectroscopic classes. Luminosity effects and scatter for II-V stars in Figure 4 are much reduced if the abscissa is instead 2980-3320, as in Figure 6. In fact, the evidence for a single sequence is strong enough to justify correcting 2980-3320 for stars that appear most discrepant. β Tri, θ Cyg, ζ Cyg, ε Cyg and α Boo are marked with underbars. If we shift these stars horizontally to fit a smooth curve

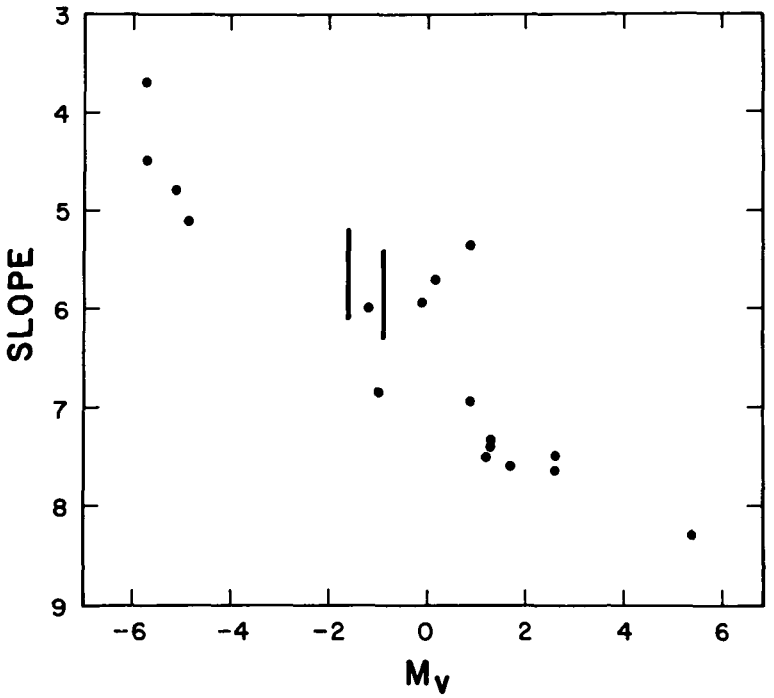

Figure 5.—SLOPE vs. Wilson and Bappu absolute magnitude. SLOPE identifies the positions of stars in Figure 4 for which B-V > 0.8.

through the remaining points, we then shift these stars vertically in Figure 3 as shown by the arrows. The result in every case improves the correlation of ultraviolet with visual color for II-V stars taken as a group.

For α Cyg there is no measurement of 2980-3320. In Figure 6 this star has been placed arbitrarily at 0.6.

Figure 7 shows 1910-V. Most of the stars with B-V > 0.9 register only a few net 1910 counts at the longest integration time. With uncertainties in DARK up to about 4 counts, errors of $\pm 0^m.5$ are likely. α Boo (B-V = 1.24) has a high count and its position should be well determined. It appears brighter than the other giants, which is not true for other wavelengths. Unfortunately, only one observation is available.

Figures 8-10 compare the OAO data for selected stars with model atmospheres from the extensive grid of models computed at the Smithsonian Astrophysical Observatory (Carbon and Gingerich 1969). These models include convective transport and statistical treatment of metal line blanketing. Models without convection and blanketing are also given. Only blanketed models are used in this comparison. The light lines represent the continuum flux, while the heavy lines are the continuum flux multiplied

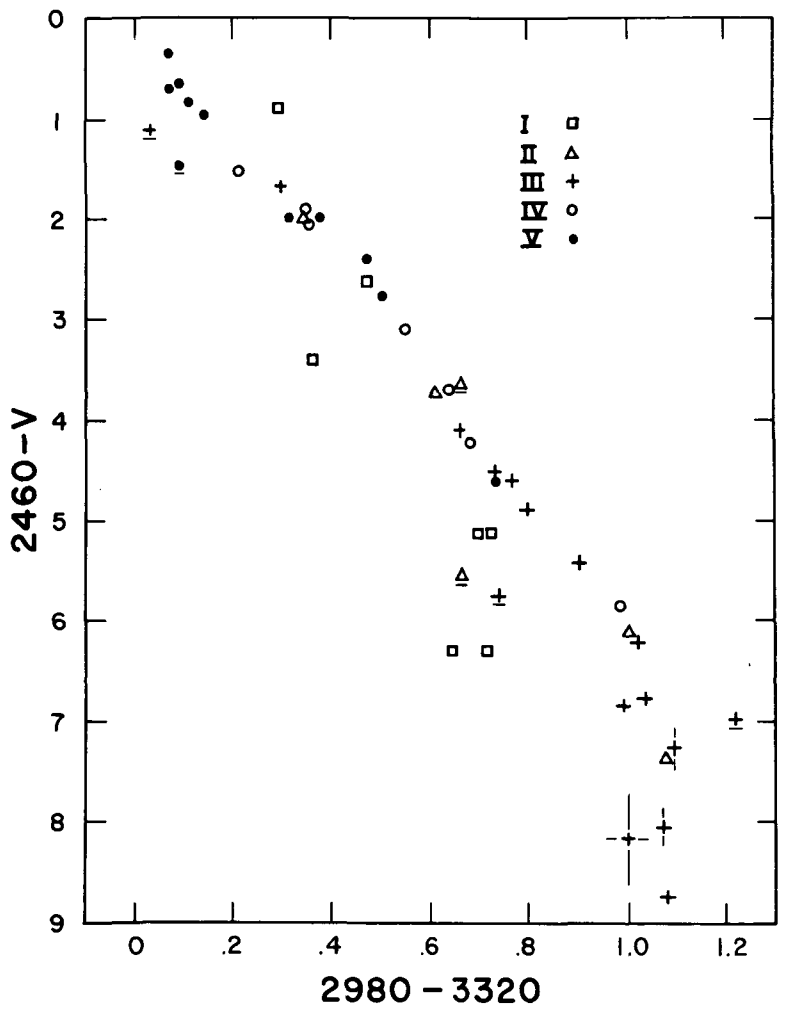

Figure 6.—2460-V vs. 2980-3320 with corrected, absolute colors. Underbars indicate observations with probable photometric errors in 2980-3320, as discussed in text.

by (1-η), where η is the tabulated blanketing coefficient. Filled circles are narrow-band observations of Mitchell and Johnson (1969) that have been calibrated against Oke and Schild's (1970) Vega measurements. Mitchell and Johnson's bands 52 and 80 were used to determine the effective temperatures of the models to the nearest 50°K. The observed and theoretical fluxes are normalized at 5180 Å.

The OAO data are plotted for two absolute calibration schemes. Open circles are based on the model atmosphere which Schild et al. (1971) fit to Vega. Crosses show the observations based on Code's calibration (Table 2). In both cases the

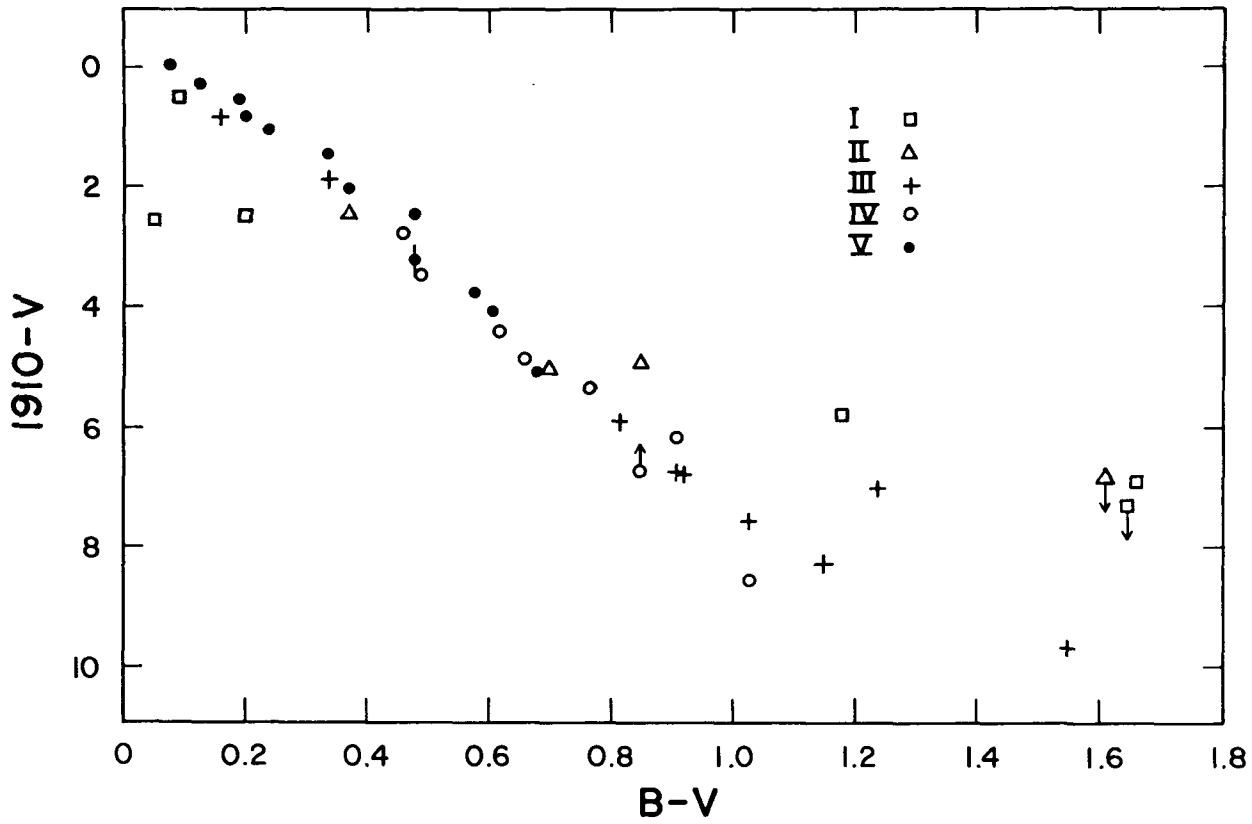

Figure 7.—1910-V vs. B-V with corrected colors and ordinate zero shift.

observed fluxes are plotted at the nominal filter wavelengths, but the fluxes have first been multiplied by the factor

$$\frac{F^{*}_{\lambda_0} \int F^{c}_{\lambda} S_{\lambda} d\lambda}{F^{c}_{\lambda_0} \int F^{*}_{\lambda} S_{\lambda} d\lambda} .$$

Here F_λ is a model flux and S_λ is the photometer response. λ_0 is the nominal filter wavelength. The superscripts * and c refer, respectively, to the models employed in Figures 8-10 and to the calibrating model (or mean model). Below 7000°K the corrections to 1910 and 2460 become substantial. The greatest correction used here is a reduction of $1^{m}.70$ in the observed flux of α Ari at 1910 Å.

The agreement between theory and observation is quite good

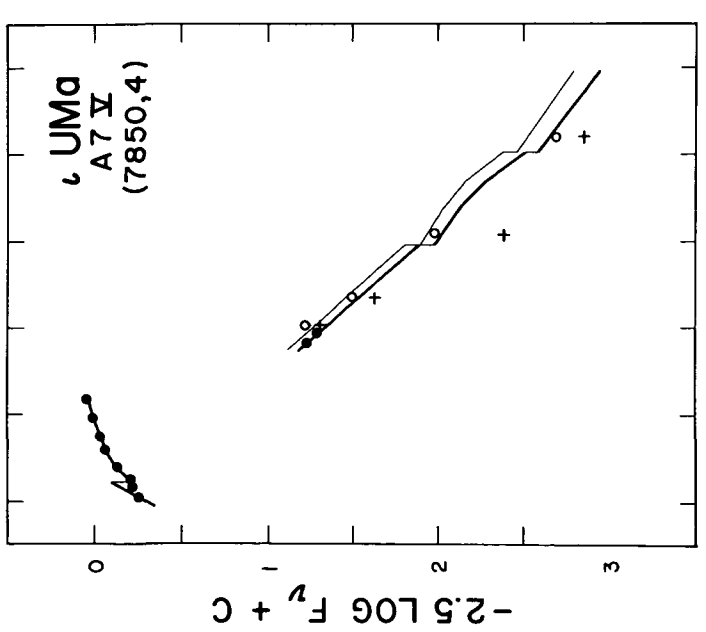

Figure 8.—Comparison of ι UMa observations with SAO blanketed model atmosphere. Filled circles, Mitchell and Johnson narrow-band data; open circles, OAO calibrated with Vega model; crosses, OAO calibrated with B star models; light line, model continuum; heavy line, model net flux.

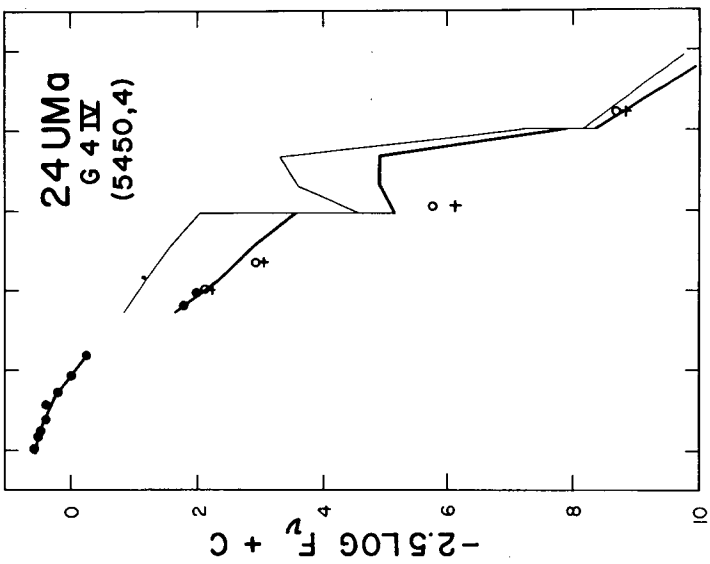

Figure 9.—Comparison of 24 UMa observations with SAO blanketed model, as in Figure 8.

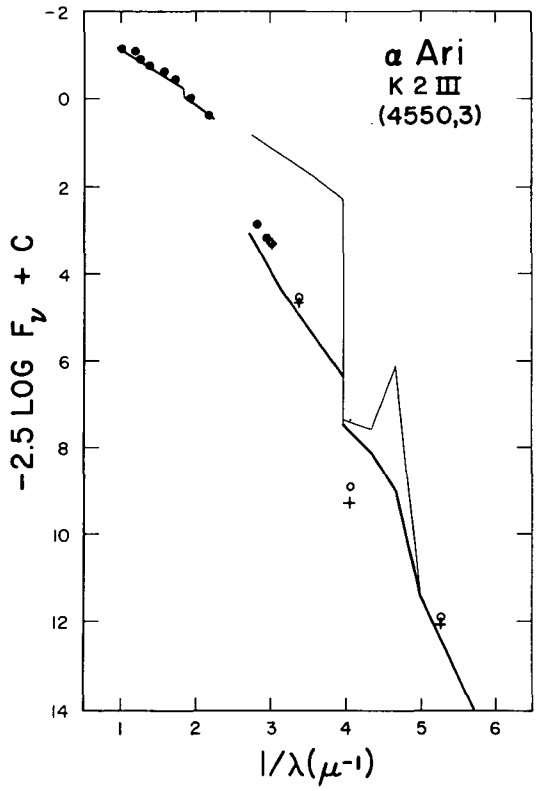

Figure 10.—Comparison of α Ari observations with SAO blanketed model, as in Figure 8.

over the entire range of wavelengths with the exception of 2460 Å. For ι UMa (7850°K), all points calibrated with the Vega model agree very well. This is not surprising, since both are ATLAS models and differences between models and stars could be nearly the same at A0 and A7. However, 2460 based on early B stars is a half magnitude fainter than the model for ι UMa and, by implication, for A0 stars also. This discrepancy increases with later spectral type. A deficiency in the neighborhood of 2500 Å is, of course, a long-standing problem in the interpretation of the solar spectrum. The origin of the required additional opacity is not known. If the B stars are also deficient at 2460 then the 2460 crosses in Figures 8-10 must be lowered even further.

I thank Dr. J. Caldwell for making his data on late-type stars available to me and Dr. R. Bottemiller for his computations of filter effective wavelengths. This research was supported by NASA NAS 5-1348 contract.

REFERENCES

Blanco, V. M., Demers, S., Douglass, G. G. and Fitzgerald, M. P. 1968, Publ. U. S. Naval Obs. (Washington: U. S. Gov't Printing Office), Vol. 21.
Bless, R. C. and Savage, B. D. 1972, Ap. J., in press.
Caldwell, J. J. 1970, Ph. D. Dissertation, University of Wisconsin.
Carbon, D. and Gingerich, O. 1969, in Proc. 3rd Harvard-Smithsonian Conference on Stellar Atmospheres, ed. O. Gingerich (Cambridge: M. I. T. Press).
Code, A. D., Houck, T. E., McNall, J. F., Bless, R. C. and Lillie, C. F. 1970, Ap. J. 161, 377.
Cousins, A. W. J. and Stoy, R. H. 1963, Roy. Obs. Bull. No.64.
Gliese, W. 1969, Veröff Astr. Inst. Heidelberg No. 22
Iriarte, B., Johnson, H. L., Mitchell, R. I. and Wisniewski, W. K. 1965, Sky and Telescope 30, 21.
Johnson, H. L. 1966, Ann. Rev. Astr. and Ap. 4, 193.
Mitchell, R. I. and Johnson, H. L. 1969, Comm. Lunar and Plan. Lab. (University of Arizona), No. 132.
Oke, J. B. and Schild, R. E. 1970, Ap. J. 161, 1015.
Schild, R. E., Peterson, D. M. and Oke, J. B. 1971, Ap. J. 166, 95.
Smithsonian Astrophysical Observatory Star Catalog, 1966 (Washington: Smithsonian Institution).
Wilson, O. C. and Bappu, M. K. V. 1957, Ap. J. 125, 661.